Multidisciplinary Optimization Strategies using Evolutionary Algorithms with Application to Aircraft Design

Artur Fouto[1], M. A. Gomes[2] and A. Suleman[3]
IDMEC-Instituto Superior Técnico, Lisbon, Portugal

This paper describes the development of a preliminary aircraft design application employing the concepts of Multidisciplinary Optimization (MDO) and evolutionary algorithms. Aerodynamics, structural analysis and flight performance are the main disciplines considered for preliminary aircraft design. Aerodynamic analysis is performed using a 3D panel method with boundary layer correction and the structural analysis is performed using a finite element method, both by external software packages handled by the developed application. A particle swarm optimizer was developed to handle the MDO problem with a large number of design variables, an Artificial Neural Network (ANN) was investigated to predict the Pareto Front (in a context of Multiobjective Optimization) and as an accelerator for the whole optimization process. The goal of developing an application that is fully independent from user input during the optimization process and is able to interact with external analysis tools was reached and several simple aircraft design optimization problems are solved, in order to demonstrate the advantages of the MDO concept and the developed optimization framework.

I. Introduction

ONE of the biggest challenges that MDO tools have to overcome is flexibility to adapt to different engineering scenarios and are usually bound to solving a predetermined set of design variables. Furthermore, the analysis fidelity level is typically low, relying on methods that are often too much simplified to deliver the much needed accuracy.

The main objective of this work is therefore to create an MDO tool that moves towards higher fidelity tools, in the context of aircraft design and integrating the emerging concept of evolutionary algorithms. In order to fulfill this requirement, a suitable optimizer has to be chosen or developed. Analysis tools that meet the desired depth level must also be chosen taking in account the balance between accuracy and computational cost. This application must be developed to interact with the analysis tools considering them as independent blocks, functioning as external modules, so that more accurate tools can be easily used in the future, simply by swapping them. Finally, the computational cost of running an optimization problem should be reasonable.

The developed application should be validated by several optimization problems, both singlediscipline but, most importantly, multidisciplinary ones, particularly in the aircraft design field.

II. Approach to MDO

Traditionally, engineering design consists of a sequence of steps, beginning with a conceptual solution to a certain mission that is to be performed. This conceptual phase continues on to a preliminary stage until a configuration can be frozen. Only then are detailed analyses performed, corresponding to each discipline involved in the "product" to be developed.

[1] MSc. Student, Departamento de Engenharia Mecânica, Instituto Suprior Técnico.
[2] Assistant Professor, Departamento de Engenharia Mecânica, Instituto Superior Técnico.
[3] Professor, University of Victoria, Department of Mechanical Eng., Victoria, BC, Canada; AIAA Associate Fellow

However, this design methodology leads to a successive bottlenecking in design freedom as the analyses and design detail is increased (Fig. 1), a fact that has been formally demonstrated[1] and that may lead to a suboptimal design, furthermore emphasizing the advantages of an MDO approach.

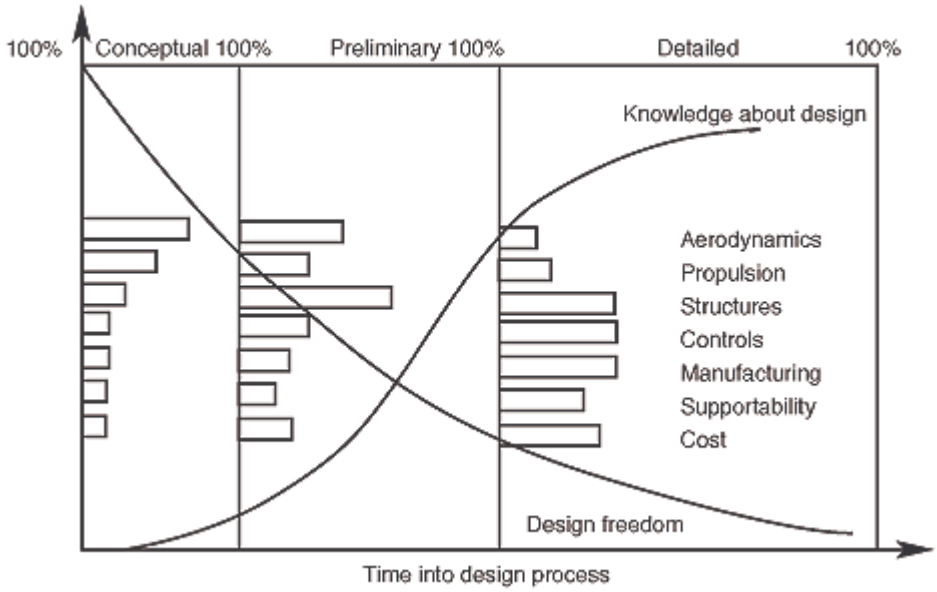

Figure 1. Traditional approach to product development.

For the purpose of this work, the following definition for MDO is considered: *"A methodology for the design of complex engineering systems and subsystems that coherently exploits the synergism of mutually interacting phenomena"*[1]. Multiple conflicting requirements have always had to be taken into account and, therefore, it can be considered that the multidisciplinary process has always been used. The key word in the definition, however, is methodology[2]. MDO provides a collection of tools and methods that permit the trade-off between different disciplines involved in the design process. *"MDO is not design but enables it"* [1].

Ideally, the MDO environment should be interactive and flexible enough to allow the problem definition, constraints to be applied and simulation depth to be fully specified by the design team, rather than the individual disciplines' teams.

In order to facilitate information exchange between the various disciplines and respective teams (or for that matter, analysis tools), a single global parametric model of the whole system should be used, from which discipline specific models can be generated[3-5]. This consistency has been shown to offer advantages, both when it comes to communication between disciplines and eventual redefinition of the global parametric model[4,6,7].

This environment should be transparent, in the sense that it should allow the design team to monitor the evolution of variables, verifying whether these are dependent or independent with relation to the problem. This enforces the notion that the top design team should have full control of the process flow.

Taking in account that modern engineering systems are extremely complex, it is only natural to distribute the various disciplines over their respective groups, all interconnected by the MDO environment. Although process distribution may present some management challenges, it truly allows for the distribution to be a physical a resource distribution, more than just a process division. This enables groups to be able to be in different sites, often worldwide; it also enables the use of computational resources and data storage spread over a vast number of nodes[8].

In this work, an intermediate level of optimization is attempted, regarding the methods used for disciplinary analysis. The structure of the MDO process is described in Fig. 2:

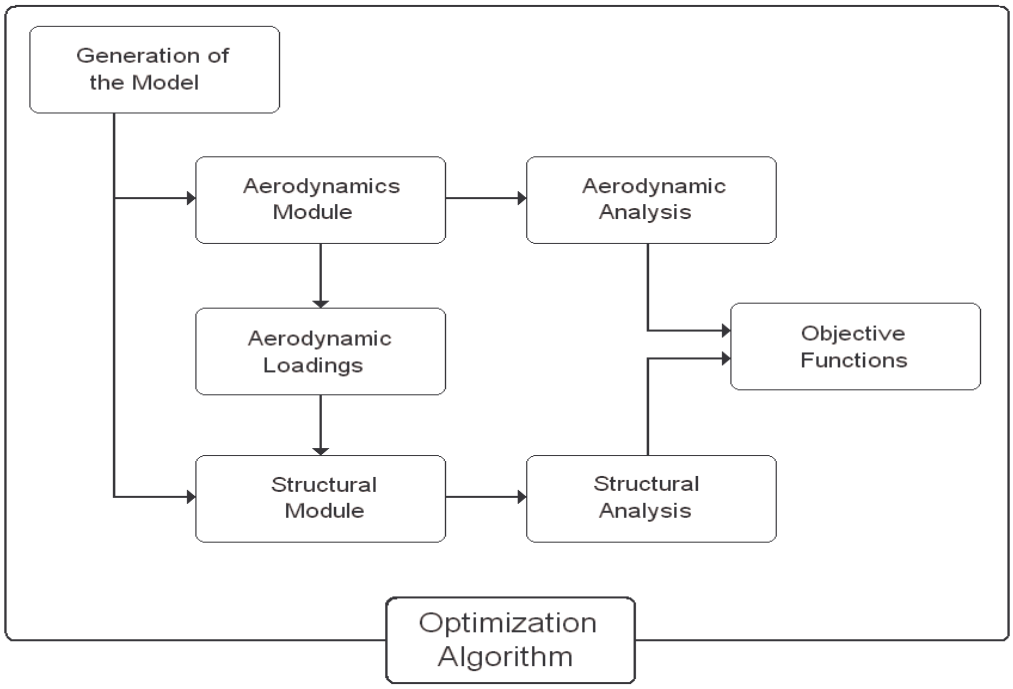

Figure 2. MDO process layout.

As seen from Fig. 2, suitable optimization algorithm and aerodynamic and structural analysis tools had to be chosen and eventually developed. Regarding the analysis tools, as a higher level of optimization was the goal and as computational resources allow, a 3D panel method with boundary layer correction was chosen for the aerodynamic analysis and finite element method for the structural analysis. The chosen optimization algorithm was the Particle Swarm, a population based algorithm, that research in the optimization field shows this method yields good results, when applied to engineering.

In the following sections of this paper, the optimization algorithm and the chosen analysis tools will be presented in further detail.

III. Particle Swarm Optimization

Being the topic of this work the development of an MDO application, a suitable optimizer needed to be chosen or developed. Taking in account the large number of design variables (DV's) resultant from the high level of detail attempted, gradient based algorithms were set aside, as these could lead to a high computational cost[9]. Using other optimization methods was also a decision made early on in this work, as only in the recent past have non gradient methods started to be explored.

As deterministic methods were set aside, the use of Evolutionary Algorithms (EA's), or for that matter, any biologic process inspired algorithms, was the chosen path to follow. Evolutionary algorithms are a set of a larger group of algorithms, so called metaheuristic methods.

In these methods, the goal is to find the extremes (from this point on assumed to be the minima) of a certain objective function with the advantage that the exact state function needs not to be known, i.e., the evaluation module(s) of a possible solution can be looked at as a "black-box". This is of extreme advantage in the design of complex engineering systems, as it would be difficult to find the function that relates the inputs (the DV's) to the output (the objective function).

The Particle Swarm Optimization algorithm was chosen, as this is a reasonably recent method and research in the optimization field shows this method yields good results, when applied to engineering[10,11].

Particle Swarm Optimization is a population-based evolutionary algorithm based on the concept of social intelligence. In this algorithm, a group of initial individuals is randomly generated, containing information about their position and velocity within a subspace of the DV's. Each individual is then evaluated by an objective function that defines which individual holds the best position in relation to the problem at hand. On the next iteration, individuals are attracted to that point as well as to their respective best position ever, by changing their velocity. As the optimization process develops, the whole population further explores the subspace and will eventually converge to the optimum of the objective function in that subspace.

This method holds a number of advantages that makes it a suitable optimizer for the problem at hand: it has advantages over other EA's, regarding efficiency (lower number of iterations needed to attain an optimal solution) and flexibility (independence from the problem to solve)[10,11]; it is a robust minima finder (for both local and absolute minima), as noise insensitivity is well shown[12-14]; it has the ability of finding a minimum outside its initial bounds; there is independence between the dimension of the space in which the particles move and the number of particles in the swarm, regarding the algorithm's ability to find a minimum and it is an obvious choice for a distributed computation environment.

Although there are many available software packages with several variations on the basic PSO algorithm, a custom version was implemented for this work, as this approach leads to a better control and adaptability to the rest of the application.

According to the heuristics behind PSO, a certain particle is moving in a hyperspace of dimension N, with current position given by x_i and velocity by v_i. Dimension, N corresponds to the number of DV's in the optimization problem and each component of the vector x_i would be the corresponding DV's value. The distance d_i between any two points is simply calculated as the difference in position between them:

$$\begin{aligned} x_i^{t+1} &= x_i^t + v_i^t \Delta t \\ v_i^{t+1} &= \omega v_i^t + C_G \frac{d_{i,Best\ individual}}{\Delta t} + C_P \frac{d_{i,Best\ position\ of\ i\ ever}}{\Delta t} \end{aligned} \tag{1}$$

Parameters C_G and C_P correspond to group and particle confidence factors, respectively. Typically, these parameters are random values that are positive and no greater than a prescribed limit (typically no greater than 3). The ratio between the two limits will determine the behavior of the swarm. If the ratio favors particle confidence, then it is most likely that an individual particle will move towards its own verified minimum, giving the algorithm good local minima search capability. On the other extreme, where higher group confidence is verified, all of the particles will tend to the global minimum, giving the algorithm a better global minimum search capability.

Parameter ω is a value comparable to the particles' inertia. Again, choosing its value should be done taking in account what is the desired behavior of the swarm. A lower inertia particle will have a greater sensitivity to local and global minima, giving the swarm faster convergence behavior. Naturally, a too low inertia will make the swarm potentially chaotic.

Typical values used throughout the work were $C_G = 2.5$, $C_P = 1.0$ and $\omega = 0.8$.

For this work, other features were added to the basic algorithm, in order to increase its stability and convergence behavior. Limiters were introduced, and greatly improved the algorithm's stability. This was done by limiting the maximum value for the particles' velocity at $v_{max} = 0.5$ for a time step of $\Delta t = 0.2$. Another feature that contributed for faster convergence was to progressively decrease the particles' inertia.

The developed algorithm was then tested against some typical benchmark functions[4], with different dimension and population size, and was found to be robust in finding local and global minima and therefore suitable to use as an optimizer for the MDO application.

As often the optimization problem is a multiobjective problem, the concept of Aggregate Objective Function is introduced. This concept allows turning a multiobjective problem into a single objective problem through the operator:

$$f_{AOF} = \sum_n a_n f_{n,singleobjective}, a_n > 0 \tag{2}$$

[4] Extended Rosenbrock, Beale and Freudenstein & Roth functions.

Prescribing the values a_n will result in the optimization process finding an optimal point. Naturally, a careful dimensional analysis should be performed *a priori* to find appropriate weights for the various singleobjective functions. This will ensure that the contribution of each singleobjective function is comparable and has relevance for finding a solution for the problem at hand.

IV. Analysis Tools

A. 3D Panel Method

As stated, a 3D panel method with boundary layer correction was chosen for the aerodynamics analyses.

Panel methods are techniques for solving potential flow. Therefore, their applicability would be reduced to incompressible flow and high Reynolds number and would fail to calculate the viscous component of the flow over the 3D body. However, after applying boundary layer corrections, calculated along streamlines of the potential flow and compressibility corrections, it is possible to achieve good accuracy outside its original bounds[15]. Computationally, its cost is much lower than that of a CFD approach (finite volume based methods), and the time per analysis allows this method to be used with the chosen optimization algorithm. Furthermore, it also allows an easy way to interact with an FEM application, as both meshes can have a common surface where aerodynamic pressure is applied to the FE model.

More simplified methods are available, such as 2D Panel Method and Lifting Line Theory[9]. However, these methods present too much simplification and the associated inaccuracy, particularly when analyzing non-lifting surfaces, such as the fuselage, which have a significant contribution to drag.

In order to use this method, an adequate panel discretization is needed for the surface of the aircraft, guaranteeing that the panels are quadrilateral, that adjacent panels share vertices and that the panels form a closed shape.

As for its implementation, the *CMARC* code was chosen, as it is already developed and validated, derived from Ames Research Center's *PMARC* code. *CMARC* conveniently creates an output file containing information on the geometry and aerodynamic coefficients at each panel, allowing for simple integration with the FE module.

B. Finite Element Method

As for the structural analysis tool, the use finite element method is widespread and allows the creation of models with as much fidelity level as wanted, from very simple models, that allow it to compete with other simplified methods (such as Equivalent Plate Theory) all the way up to high fidelity models with high geometric complexity. It also allows to directly applying the aerodynamic results (panel pressure and friction) to the shell elements on the FE model.

For this work, *Ansys*® was chosen, as it is a very complete package from mesh generation to element types available to a fast matrix solver. Furthermore, it can be fully controlled through the command line with the use of an input file declaring all actions to be taken. This is a key feature for both chosen tools, as the application described in this work is intended to be fully automatic and independent from external input.

V. Parametric Model

Typically, a geometry is first created and only then is the discretization done, defining global and local refinements in order to generate the panels and wake lines. A different approach was taken here, being a parameterization created for typical aircraft macro-components, such as the wings, stabilizers and fuselage. For a certain parameterization, i.e., a certain aircraft shape, all of the panels are then declared in a file format accepted by *CMARC*. Some care had to be taken in the declaration of the input file, as the orientation of the panels defines which side of the panel corresponds to the external flow.

For wing-like elements, parameters span, chord, dihedral, incidence, sweep and thickness are DV's (see Fig. 3). Span is a one-dimensional DV, whereas all the other are given by a function:

$$DV_i = \sum_k^p a_k f_k\left(\overline{s}\right), \overline{s} = \frac{s}{Span} \tag{3}$$

where f_k are polynomial functions of degree k, with p as the maximum polynomial degree, and dependent on the nondimensionalized span, $\bar{s}$ (s is the local span value and *Span* is the full span that the element will have). The higher the degree p, the higher the variation the parametric model can suffer.

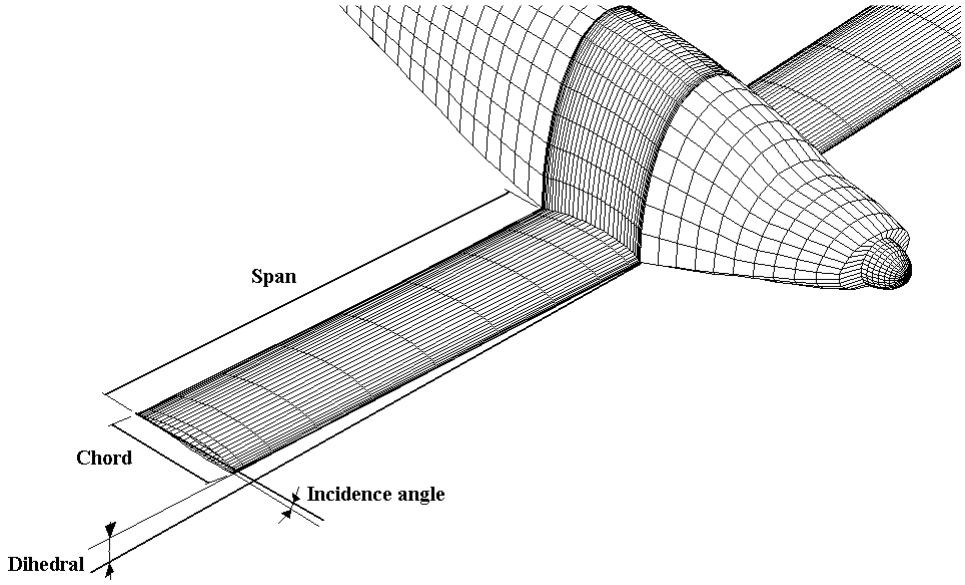

Figure 3. Design Variables for wing elements.

This approach can be extended to any other element of an aircraft, provided that a suitable parameter is chosen (in the case of a fuselage, the longitudinal distribution of cabin diameter would be an example of this). This method also presents some advantages, as it makes possible for the DV's to assume different values in any point of the element using the same number of parameters a_k, regardless of the refinement of the discretization, i.e., number of panels, in the case of the aerodynamic solver.

All the parameters a_k for all the DV's will correspond to the values in the optimization vector x_i in Eq. (1).

For example, regarding the wing (and for that matter, any wing like element, such as stabilizers or winglets), the parameterization starts with span and the airfoil, which, in this work, is not a DV, but imposed *a priori* for each lifting surface, for simplicity. The airfoil is read from a file, being this a nondimensionalised airfoil, with unit chord. Then, the other DV's are calculated from Eq. (3):

$$\begin{aligned} f_1 &= \bar{s} \\ f_2 &= -4\left(\bar{s}\right)^2 + 4\left(\bar{s}\right) \\ f_3 &= 16\left(\bar{s}\right)^3 - 24\left(\bar{s}\right)^2 + 8\left(\bar{s}\right) \\ &\vdots \end{aligned} \tag{4}$$

As can be seen from the above, f_k, for $k > 1$, are polynomials constructed in the interval [0,1], in such a way that for $\bar{s} = 0$, $\bar{s} = 1$, $f_k = 0$.

Replacing a_k with x_k in Eq. (3):

$$
\begin{aligned}
Chord_j &= Chord_0 + \sum_{k=1}^{p} x_k f_k\left(\bar{s}\right) \\
Dihedral_j &= Dihedral_0 + \sum_{k=1}^{p} x_{k+p} f_k\left(\bar{s}\right) \\
Incidence_j &= Incidence_0 + \sum_{k=1}^{p} x_{k+2p} f_k\left(\bar{s}\right) \\
&\vdots
\end{aligned}
\tag{5}
$$

The values $Chord_0$, $Dihedral_0$, $Incidence_0$, etc., are needed for a correct parameterization, as they define the DV's values at span $\bar{s} = 0$ (they correspond to using the polynomial forms above, Eq. (3), starting at $k = 0$). The distribution of the nondimensional span can be done according to the needs, i.e., in the case of wings where a fuselage exists, a full cosine distribution was used; if a *Blended Wing Body* type of aircraft was being modeled, a half cosine distribution would be the most adequate.

In Fig. 4, an example is given for the parameterization, where sweep (corresponding to the coordinates of the leading edge) and chord determined in function of span are shown and the result, in terms of panels for the aerodynamic solution. A similar process is also done for incidence, dihedral and the airfoil thickness (for a value of 1.0 the airfoil suffers no modification, other values will thin or thicken the airfoil).

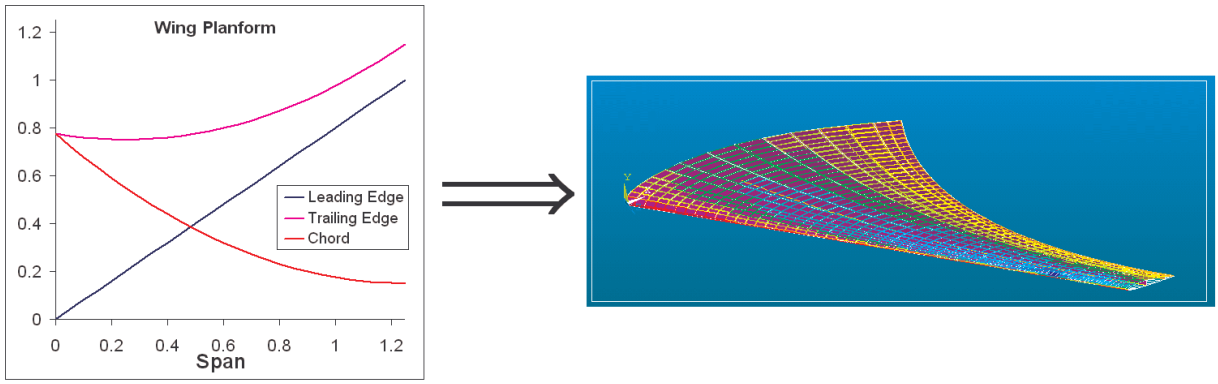

Figure 4. Example of Parameterization.

Naturally, bounds can and should be applied to any of the DV's, so that any physical imposed constraints are transported onto the aerodynamic model. Even if no physical constraints are to be added, it is a good practice to apply them, in order to avoid generating a model that would have severe geometric distortion to the point where numerical convergence issues of the solution could appear.

This parameterization philosophy can be extended to the structural elements. For beams, for example, a section geometry can be assumed (I-beam, T-beam, etc.) and parameterized to a single parameter. For shell thickness, this method was extended to a bidimensional parameterization to allow variations along any direction.

VI. Results

In this section, the results obtained with the application are shown. The first two optimization problems are simple problems, aimed at observing the behavior of the application, regarding the optimization algorithm's capability of handling a real life problem and guaranteeing that the interaction with the external modules is seamless. The two following problems are more complex, with a larger number of DV's to be optimized and integrated in the aircraft design environment. Finally, a true MDO problem is solved, as the previous problems are singlediscipline (only aerodynamic or structural).

A. Simple Aerodynamic Problem

In this first example, a simple aerodynamic optimization problem is explored. A rectangular wing is to be optimized, regarding its spanwise incidence distribution. Span, chord and airfoil are predefined and constant

throughout the optimization process. Wing semispan is *5* m and chord is *1.25* m. The chosen airfoil was a NACA 63A612, which has maximum C_l/C_d at an angle of attack of *3*º [5]. Incidence angle at the wing root was set at *5*º on purpose, in order to have convergence to a solution other than a predictable optimal elliptical distribution of C_L and the analysis made at a null angle of attack. Bounds were imposed on maximum and minimum local incidence angle at *-6*º and *+6*º, respectively. The objective function for this problem was simply given by the function:

$$f_{L/D} = -\frac{C_L}{C_D} \tag{6}$$

In this case, the wing was discretized with 40 panels spanwise, with a cosine spacing (greater refinement near the wing tip). As the purpose was to test the capabilities of the optimizer, the swarm population was set to 6 individuals (due to the small number of parameters to be optimized), 15 iterations were performed and the aerodynamic solution was performed without boundary layer correction.

Table 1 compares a constant incidence wing (*5*º throughout the whole span), the best initial solution, i.e., the best random individual in the initial population and the final best solution in the population; the increase in *L/D* ratio in relation to the constant incidence wing is shown.

	L/D	to Constant Incidence
Constant Incidence	29.42	-
Best Initial Solution	40.26	+ 36.8%
Best Solution	45.10	+ 53.3%

Table 1. Table of Gains from the optimization process.

Spanwise distribution of incidence of the best solution obtained is shown in Fig. 5. The evolution of the optimization process is shown in Fig. 6, with points representing each individuals score at each time step, as well as lines representing the evolution of the average and best value of the objective function.

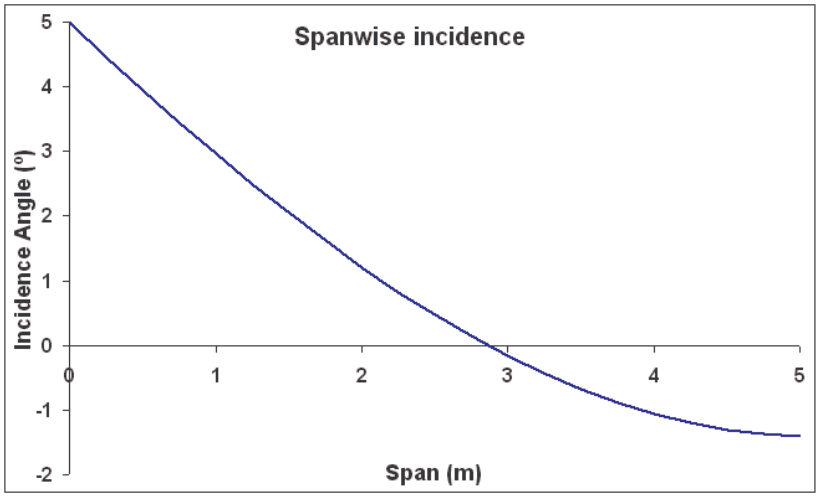

Figure 5. Spanwise distribution of incidence.

[5] Obtained through *XFoil*, for *Re = 4M*, *5M*, with $C_l/C_d \approx 170$.

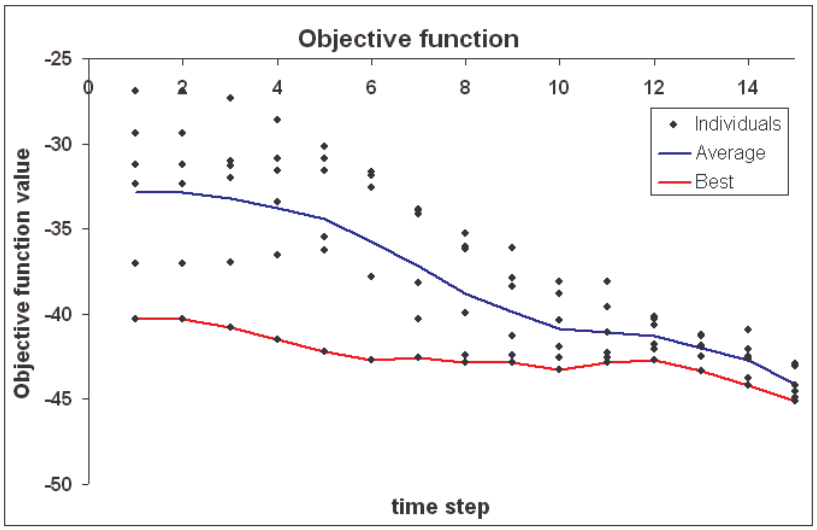

Figure 6. Optimization process evolution.

From the results above, it can be concluded that the optimizer was capable in the context of this problem. As expected, incidence distribution is such that the incidence angle decreases towards the wing tip, down to a negative angle. Being the wing's planform a rectangular one, this is to be expected, as the induced circulation will lead to an effective angle of attack at the tip higher than that of the free-stream. The solution also presents a high variation of incidence in the root region, also to be expected, as the root incidence was set to *5*º, a higher value than the airfoil's optimal C_l/C_d point.

B. Simple Structural Problem

In this example, a simple structural optimization problem is explored. An aluminum I-beam is optimized regarding its web height along its span. Height is defined in the z direction. The geometry of this beam and its loadings is shown in Fig. 7.

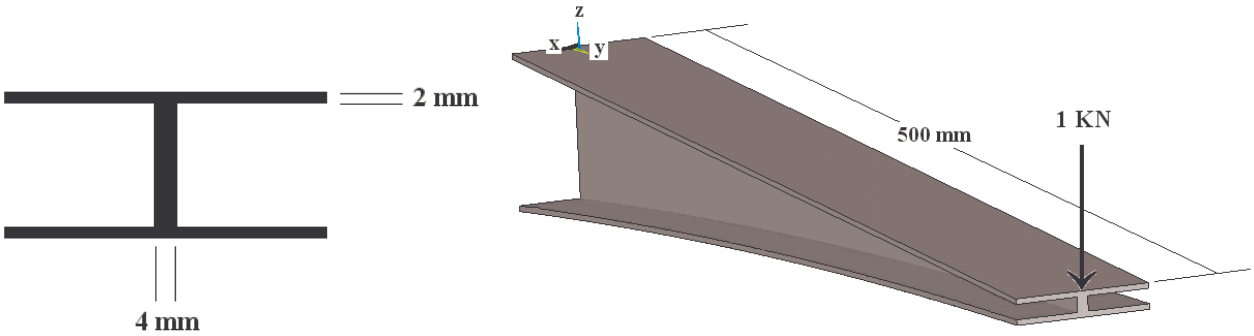

Figure 7. Beam section and geometry.

Bounds were imposed on maximum and minimum height of the beam's web, *5* mm and *70* mm, respectively.

As for the solution to be achieved, the objectives to be satisfied are low weight and maximum stress lower than a prescribed limit. Thus, the objective function was constructed as follows:

$$f_{Objective} = f_{mass} + f_{Average\,Stress} + f_{\sigma_{max}} \tag{7}$$

where

$$f_{mass} = 25\, m_{beam}\,,$$

$$f_{Average\,Stress} = \frac{\sigma_{max} - \sigma_{avg}}{10}$$

$$f_{\sigma_{max}} = \begin{cases} 0, \sigma_{max} \leq 100MPa \\ 100\left[\frac{\sigma_{max} - 100MPa}{100}\right]^2, \sigma_{max} > 100MPa \end{cases}$$

Regarding the first objective, both mass and average stress are considered: f_{mass} naturally penalizes a solution with high mass, whereas $f_{Average\ Stress}$ will benefit a solution that has equal stress in the beam's cap (where this function is analyzed, as higher stresses are expected in this region). As for the function regarding maximum stress, this highly penalizes solutions with stresses above the prescribed admissible stress, in this case chosen as *100* MPa.

For this problem, the beam was discretized with 960 shell elements (320 for each of the caps and web), the swarm had 8 individuals and 20 iterations were run. Table 2 compares the best initial solution, i.e., the best random individual in the initial population and the final best solution in the population regarding their objective function value, mass, maximum stress and average stress.

	Objective Function	Mass (kg)	σ_{max} (MPa)	σ_{avg} (MPa)
Best Initial Solution	16.34	0.523	74.7	42.2
Best Solution	11.04	0.399	102.1	91.9

Table 2. Table of Gains from the optimization process.

Fig. 8 shows the web height distribution along the beam span. As expected in a problem of this sort, the solution shows an almost linear variation, reaching, at the beam tip, a value that was naturally determined by the lower bound imposed on this parameter (*5* mm).

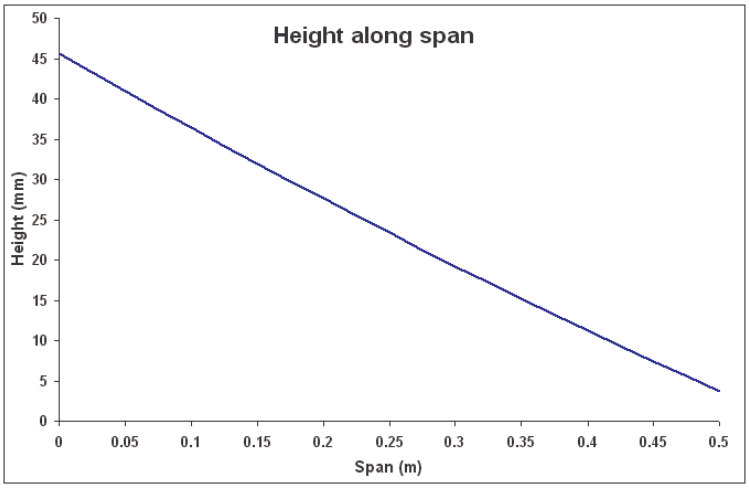

Figure 8. Height distribution along span, for the final solution.

Figures 9 and 10 show the stress distribution on the upper spar cap (subject to tension). It clearly shows the effect of having a component in the objective function that benefits solutions where this element is stressed in a uniform way. It should also be noted that the maximum stress in the structure is slightly higher than wanted by *2 %*. This can be explained as the objective function is continuous and reflects the care that must be taken when designing "penalty" functions such as this one.

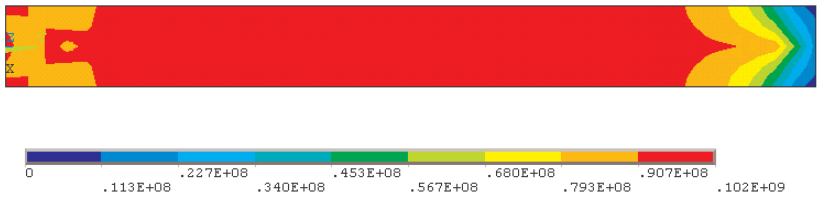

Figure 9. Stress in the upper cap (unit *Pa*).

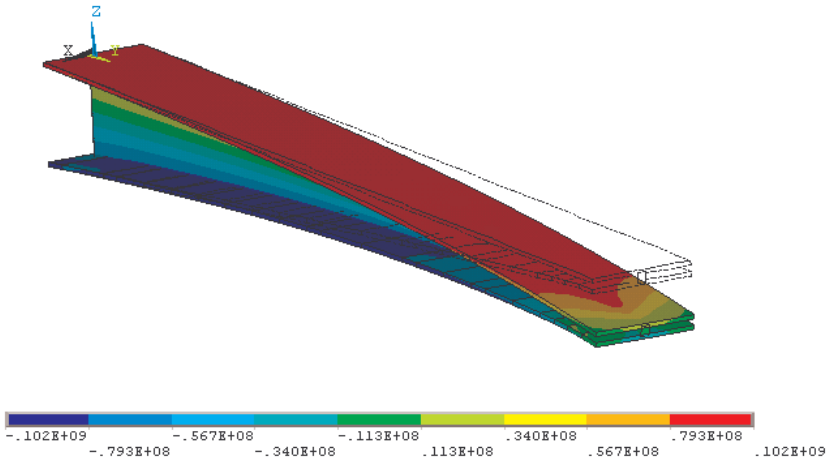

Figure 10. Final solution (σ_{yy}, unit *Pa*, scale 2:1).

Finally, figures 11 and 12 show the evolution of the objective function and mass for this optimization problem. Looking at both graphs, it should be noted that, initially, a large number of individuals have very high objective function values, mainly due to maximum stress being higher than the allowed. As the optimization process goes on, all of the individuals start approaching the optimum (iterations 8 to 15). Then, higher values start appearing again, fact that is explained by the fact that all solutions now have a geometry that leads to low mass but, therefore, also high stresses.

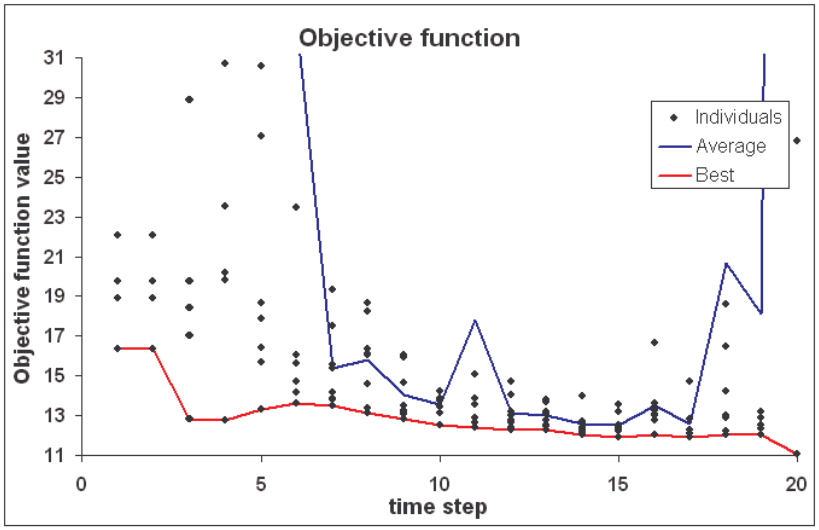

Figure 11. Optimization process evolution.

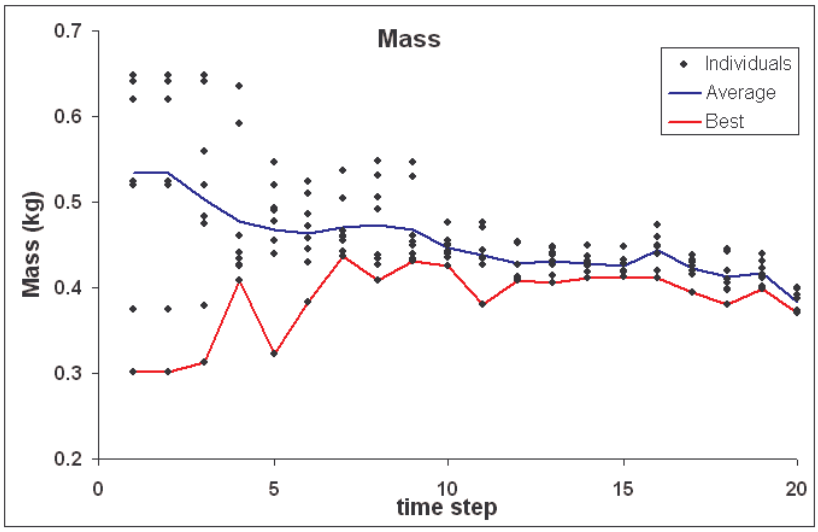

Figure 12. Beam mass evolution.

C. Winglet Optimization

In this problem, a full aircraft without winglets is modeled and analyzed, in order to establish a baseline solution. This aircraft model is inspired in dimensions on a typical two-seater light airplane and was designed in a way that it is statically stable and has an approximately elliptical *Lift* distribution. The results for this baseline configuration are shown in Fig. 13.

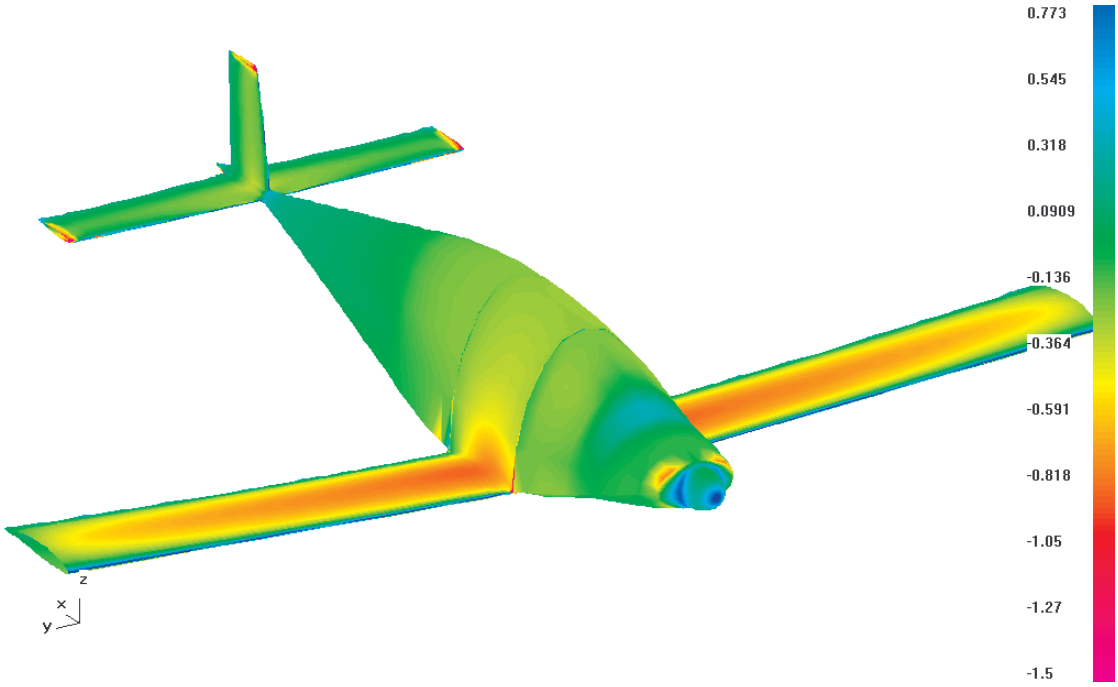

Figure 13. C_P distribution on the baseline aircraft.

Then, the model in Fig. 13 is used, but winglets are added and optimized. These winglets have some constraints (maximum span and area) but are otherwise allowed to have any possible shape, within the parameterization's capabilities. The objective to be fulfilled is naturally to increase the baseline model's *L*/*D* ratio, without changing the C_M of the aircraft. Maintaining C_M as close to null as possible guarantees that no extra drag will be generated by the

horizontal stabilizer, while trying to maintain static stability of the airplane. This results in the following objective function (in a way that the baseline model has a null value when evaluated):

$$f_{Objective} = f_{L/D} + f_{C_M} + f_{Winglet\ Area} \tag{8}$$

where

$$f_{L/D} = -\left(\frac{C_L}{C_D} - 25.62\right),$$

$$f_{C_M} = \left|C_M\right|,$$

$$f_{Winglet\ Area} = \begin{cases} 0, Winglet\ Area \le 0.17 \\ \left[100\left(Winglet\ Area - 0.17\right)\right]^2, Winglet\ Area > 0.17 \end{cases}$$

In order to have a shorter time for convergence, the number of iterations was limited and no boundary layer correction was used, which leads to lower drag than in reality. However, as can be seen from the results in Table 3, the greatest verified difference is in *Lift*, which would not be very affected by this component.

	Baseline	With Winglets	Variation
Lift (N)	4732	5099	+7.8%
L/D	25.6	27.9	+9.0%
C_m	0	-6.3×10^{-4}	-

Table 3. Table of Gains from the optimization process.

Furthermore, the improvement in *L/D* would have been greater if the aircraft was allowed to vary its angle of attack in order to maintain constant lift, as this would lead to a lower component of induced drag. However, as the purpose was validation of the optimization process, this simpler approach was taken. The fact that the baseline model presents an almost elliptical distribution of C_L also contributes to the relatively small improvement.

In Fig. 14, the evolution of the optimization process is shown, where the objective function value is shown for each of the six individuals in the swarm during the prescribed eight time steps.

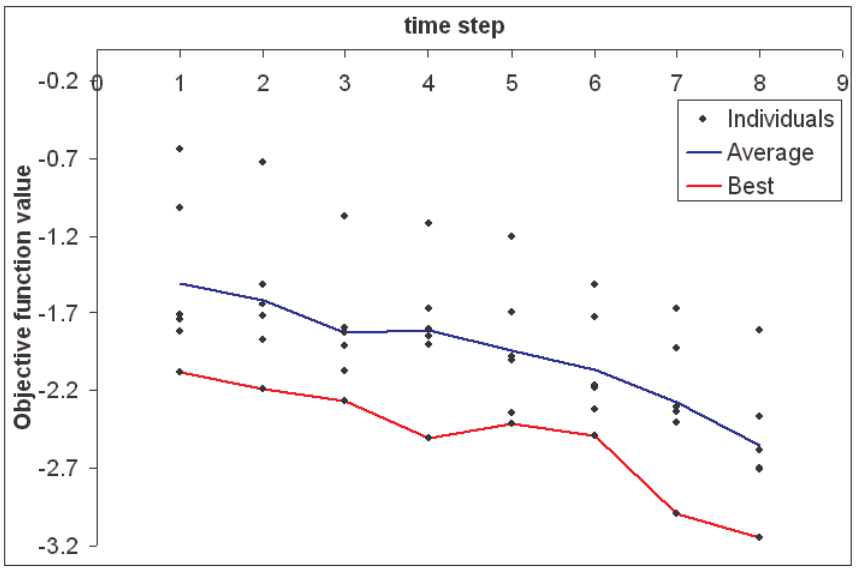

Figure 14. Optimization process evolution.

It should be noted that the winglet may appear not to be a truly feasible solution for structural reasons (see Fig. 15). But being this an aerodynamic optimization only, a structural analysis was not included, which could eventually lead to a more traditional looking winglet, without the accentuated forward sweep.

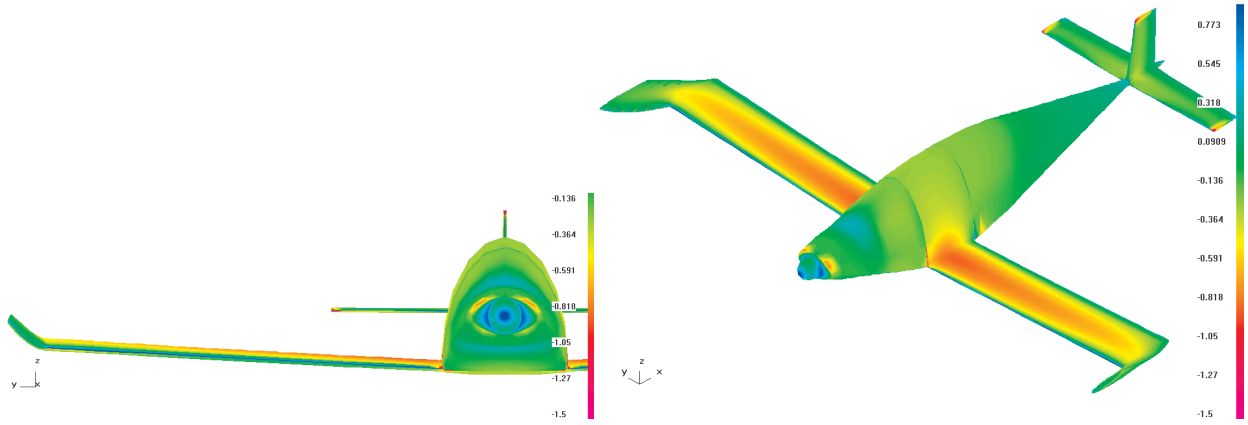

Figure 15. Resulting winglets.

D. Skin Thickness and Wing Ribs Optimization

In this problem, the aerodynamic baseline solution is used and a structural optimization is performed. Skin thickness is optimized in the whole aircraft as well as rib parameter.

As for the aggregate objective function to be minimized, several solution components were analyzed and included in it: mass, wing tip rotation, wing tip deflection and maximum verified stress.

Structural mass is obviously a main factor in aircraft design and must be minimized. Wing tip rotation was equally considered in the objective function, as a structural solution that shows significant wing torsion will have its aerodynamic solution invalidated (a true fluid-structure interaction was not used in this work). Wing tip deflection was included so that the solution is penalized if it is larger than *5 %* of the semispan. The same principle applies for maximum stress in the structure, if this value is higher than the maximum value for the considered material.

$$f_{Objective} = f_{mass} + f_{Wing\ Tip\ Rotation} + f_{Wing\ Tip\ Deflection} + f_{\sigma_{max}} \tag{9}$$

where

$$f_{mass} = \frac{mass}{10},$$

$$f_{Wing\ Tip\ Rotation} = 100\left|Wing\ Tip\ Rotation\right|,$$

$$f_{Wing\ Tip\ Deflection} = \begin{cases} 0, \delta_{tip} \le 0.2 \\ \left[25\left(\delta_{tip} - 0.2\right)\right]^2, \delta_{tip} > 0.2 \end{cases}$$

$$f_{\sigma_{max}} = \begin{cases} 0, \sigma_{max} \le \sigma_{adm} \\ 10\left[\sigma_{max} - \sigma_{adm}\right]^2, \sigma_{max} > \sigma_{adm} \end{cases}$$

Some constraints were also applied, regarding the minimum allowed thickness, as very thin shells may be unfeasible. Therefore, the minimum bound applied was *0.635* mm.

The evolution of the objective function value is shown in Fig. 16. The optimization process evolved as expected, minimizing mass (see Fig. 17) – the main contribution to the AOF – while maintaining the optimal solution within the applied constraints, as shown in Fig. 18, where wing tip displacement for the best individual in each time step is highlighted.

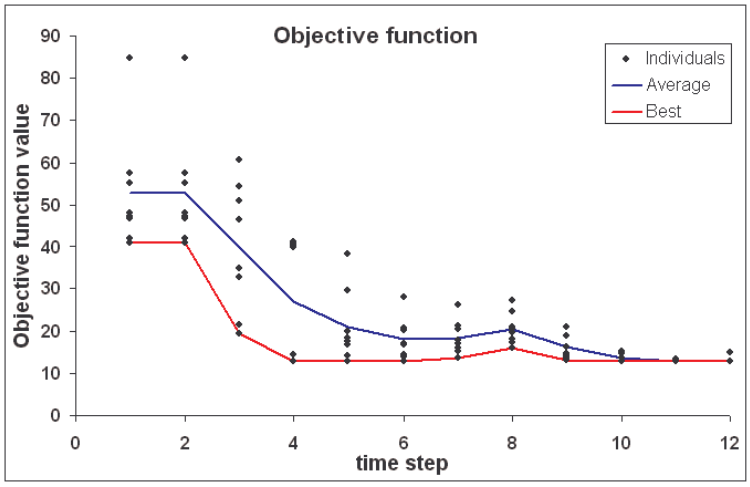

Figure 16. Objective Function value evolution.

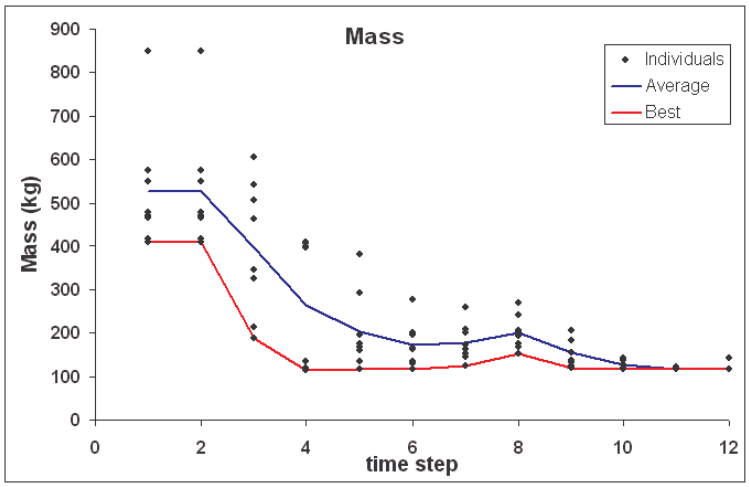

Figure 17. Mass evolution.

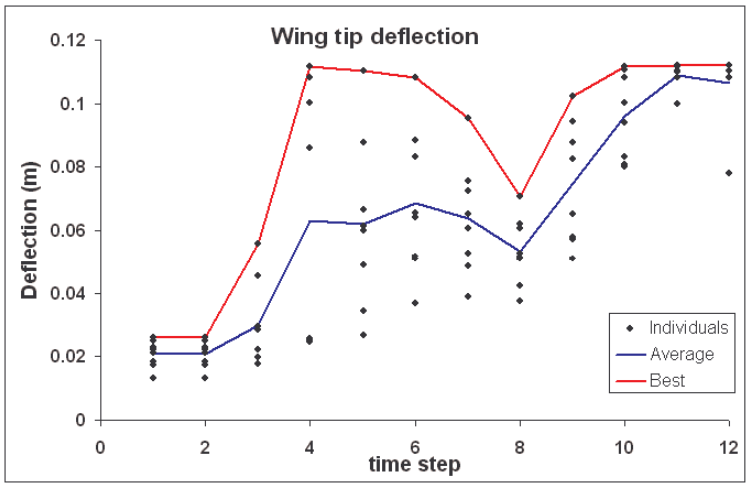

Figure 18. Wing tip deflection evolution.

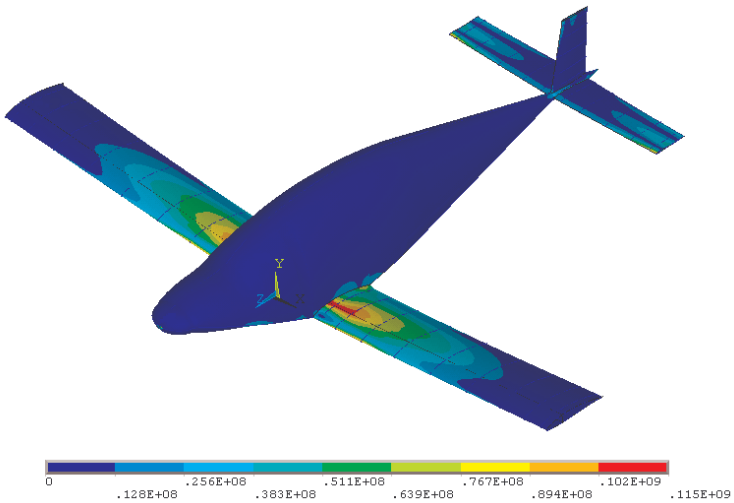

Figure 19. Stress Intensity obtained through FEM (unit *Pa*).

Stress intensity verified in the wing root vicinity, as shown Fig. 19, is above the prescribed maximum. This is not a fault in the optimizer's capabilities, but serves to show that the construction of objective functions should be done carefully. The optimal point for this particular AOF is one that gave too much value to a low mass, therefore partly sacrificing other constraints, in this case, maximum structural stress.

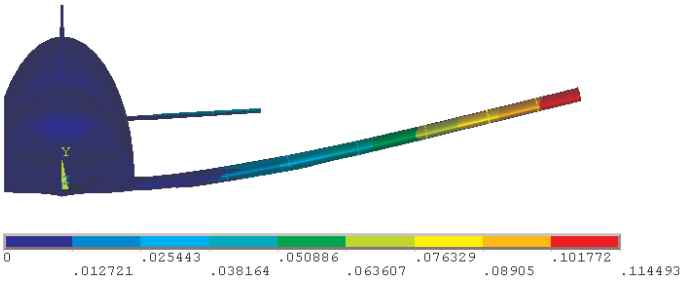

Figure 20. Wing deflection (unit *m*, scale *5:1*).

E. Multidisciplinary Optimization

Finally, a true multidisciplinary optimization problem was solved. For this problem, aerodynamics, structure and basic flight performance were analyzed. A simple scenario was created for a small surveillance UAV: a flying wing platform, with a central thicker "body", designed for long range, flying at an altitude of *5000* m and speed of *70* m/s. The geometry of this aircraft is presented in Fig. 21. In order to simplify the problem, the aircraft has a fixed span and sweep angle, $\Lambda = 27º$, and the central body has a fixed geometry. Airfoil was also constant throughout the span (except for thickness variations) and is a *Wortmann FX 69-H-098*. This airfoil was chosen for its low C_{m0} (zero lift pitching moment) as the aircraft is tailless. However, this is not a reflex airfoil and therefore is not a natural choice for this planform, regarding the aircraft's static stability. This choice was made on purpose to see the optimizer's capability to create a stable configuration even with this airfoil. Chosen geometry values are shown in table 4.

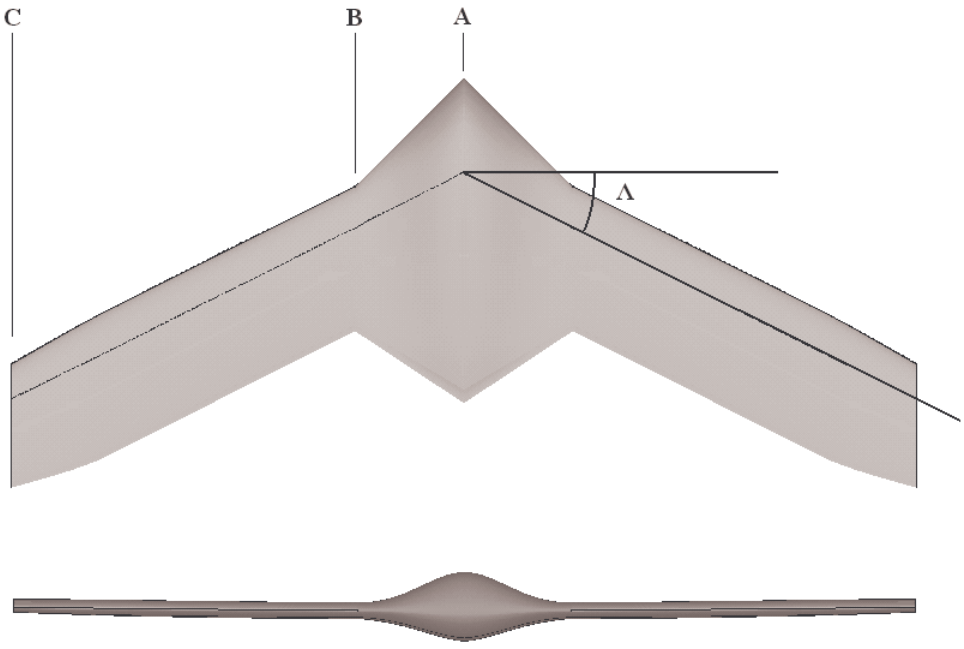

Figure 21. MDO problem: aircraft geometry.

	Chord (m)	Incidence (º)	Thickness	Distance from root (m)
Station *A*	1.80	4.0	20 %	0.00
Station *B*	0.80	3.0	10 %	0.60
Station *C*	*variable*	*variable*	10 %	2.50

Table 4. Aircraft geometry dimensions.

Regarding the aerodynamics, chord and incidence in the "wing" (between stations *B* and *C*) were the DV's to be optimized. Dihedral and sweep were left out of this problem, as only a thorough flight stability analysis would be able to resolve these parameters. As for the structure, beams were simulated by adding their respective beam web at *25 %* and *75 %* of the airfoil, being that the wing skin serves as their caps, which approaches a box-wing like construction and aluminum was chosen for material. As in section D of this chapter, skin thickness of the panels was the parameter to be optimized.

Table 5 summarizes the lower and upper bounds that were applied both to aerodynamic and structural DV's. Recalling Eq. 3, and taking in account that $p = 2$, this represents a total of 13 parameters a_k that were optimized.

Design Variable	Lower bound	Upper bound
Chord	0.10 m	0.80 m
Incidence	- 5.0 º	+ 5.0 º
Panel thickness	0.635 mm	20 mm

Table 5. Aircraft geometry dimensions.

The main objective to be fulfilled by this aircraft is long range. This result was calculated by the Breguet range equation:

$$R = \frac{\eta}{SFC}\frac{L}{D}\ln\left(\frac{W_i}{W_f}\right), \tag{10}$$

where η is propulsive efficiency (a propeller propulsion was assumed, with η = 0.8), *SFC* is specific fuel consumption (here assumed to be 0.35 $kg \cdot kW^{-1} \cdot h^{-1}$), W_f and W_i are the weight of the aircraft at the final and initial points of its mission. W_i was calculated from the lift obtained by the aerodynamic solution and W_f was estimated by assuming a *20 %* fuel fraction of the non-structural weight, derived from the structural solution:

$$W_i = \frac{L}{g}, \quad W_f = W_i - m_{fuel} = 0.8W_i + 0.2m_{structure} \tag{11}$$

The objective function was therefore constructed to evaluate each solution primarily for its range, but also included penalty functions to guarantee that wing tip displacement and rotation, maximum stress in the structure and pitching moment were within limits, in an approach similar to what is expressed in Eq. 9. A penalty is added to the objective function if wing tip rotation is not null, if wing tip deflection is greater than *5 %* of semispan, if maximum stress is greater than *100* MPa and if pitching moment is not null (choosing that the center of gravity of the aircraft is at *60 %* of root chord). Eq. 12 shows the weights given to each of these functions.

$$f_{Objective} = f_{Range} + f_{Wing\,Tip\,Rotation} + f_{Wing\,Tip\,Deflection} + f_{\sigma_{max}} + f_{C_M} \tag{12}$$

where (*Range* is in km, wing tip rotation in rad, deflection in m, stresses in MPa and pitching moment in Nm):

$$f_{Range} = -\frac{Range}{20},$$

$$f_{Wing\ Tip\ Rotation} = 100\left|Wing\ Tip\ Rotation\right|,$$

$$f_{Wing\ Tip\ Deflection} = \begin{cases} 0, \delta_{tip} \le 0.125 \\ \left[20\left(\delta_{tip} - 0.2\right)\right]^2, \delta_{tip} > 0.125 \end{cases}$$

$$f_{\sigma_{max}} = \begin{cases} 0, \sigma_{max} \le \sigma_{adm} \\ 200\left[\frac{\sigma_{max} - \sigma_{adm}}{100}\right]^2, \sigma_{max} > \sigma_{adm} \end{cases}$$

$$f_{C_M} = 2\left(\frac{M_y}{50}\right)^2$$

The evolution of the objective function value is shown in Fig. 22. The optimization process evolved as expected, maximizing range (see Fig. 23) – the main contribution to the AOF – while maintaining the optimal solution within the applied constraints (these are not shown here as the limits are being respected and such graphs would add little to this discussion).

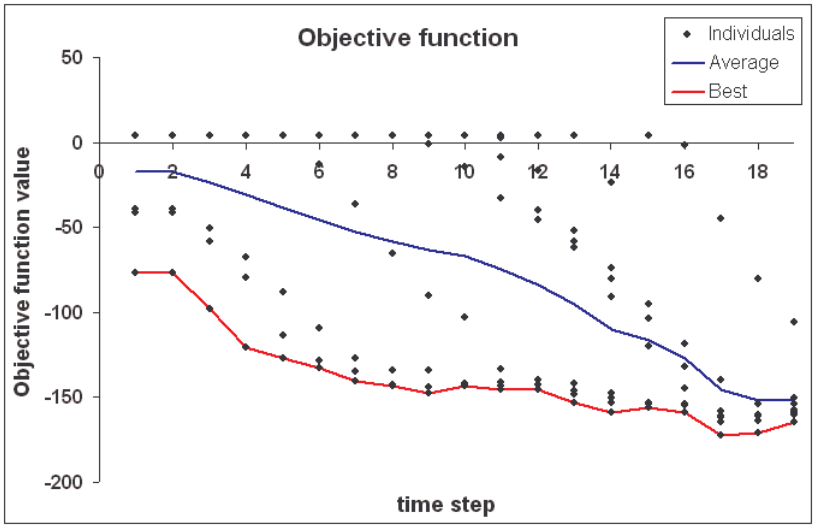

Figure 22. Objective Function value evolution.

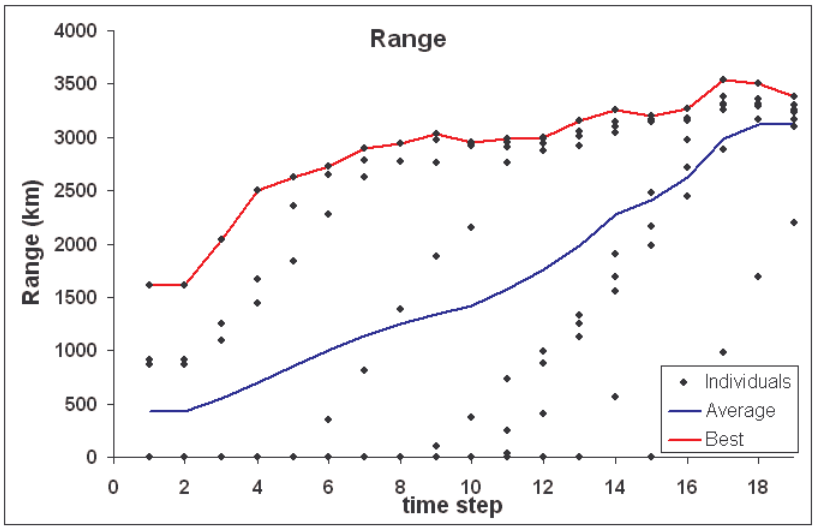

Figure 23. Range evolution.

Table 6 compares the best initial solution, i.e., the best random individual in the initial population and the final best solution in the population regarding Range, Lift, *L/D*, structural mass, maximum stress, payload (here defined as weight other than structural mass and fuel) and objective function.

	Best Random Individual	Final Solution	Variation
Range (km)	1613	3537	+119 %
Lift (N)	3054	2738	-10.3 %
L/D	21.3	22.9	+7.5 %
$m_{structural}$ (kg)	177	44.3	-75 %
Payload (kg)	108	188	+74 %
σ_{max} (MPa)	15	103	+587 %
Ojective Function	-76.6	-172.5	+125 %

Table 6. Table of Gains from the optimization process.

From the analysis of these values, it is clear that there was optimization in both aerodynamic and structural fields but most importantly, optimization in a coupled environment. Analyzing only aerodynamic performance in lift and *L/D* ration shows two similar solutions but their differences arise when data on structure is included. The optimized solution shows a maximum stress value very close to the allowed maximum, guaranteeing that the structure is capable of handling the aerodynamic loads, yet light enough to allow for a long range.

The other important results of the optimized solution are a wing tip rotation of *0.12*º, low enough not to influence the aerodynamic solution (as no coupled aero-structural analysis is performed), a wing tip deflection of *31* mm and a pitch down moment of *70* Nm (although not null, for an aircraft of these dimensions and mass it is very low, being easily compensated by control surfaces or slight shift of the center of gravity).

Fig. 24 shows the stress intensity on the optimized solution. As expected, the wing root area shows higher stresses than the rest of the structure. Fig. 25 shows the thickness distribution from which the FEM solution is obtained.

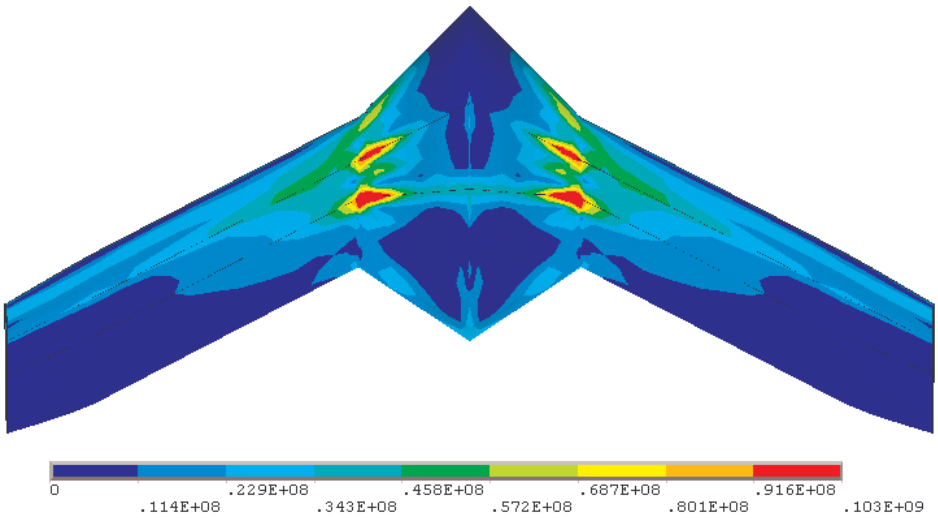

Figure 24. Stress intensity in the skin panels (top view; unit Pa).

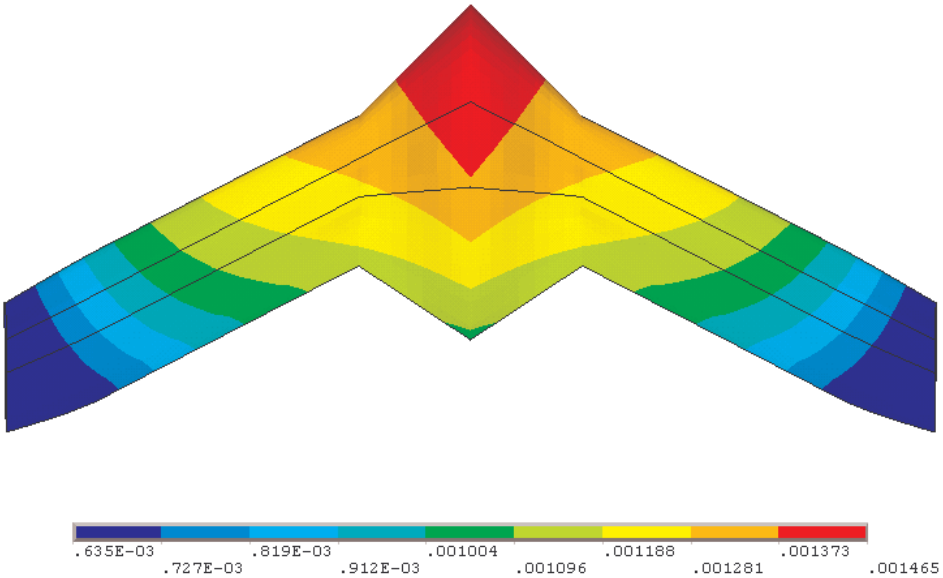

Figure 25. Thickness distribution in the skin panels (top view; unit m).

Figures 26 and 27 show spanwise chord and incidence distribution. As can be seen in the chord distribution graph, chord is almost constant throughout the wing. Even though this does not favor the best *L*/*D* ratio, it adds area to the wing, having a more significant effect on range (by means of a higher fuel mass) than another distribution. Regarding incidence, the graph shows a decreasing towards the wing tip, which favors not only the *L*/*D* ratio (by means of a more favorable lift distribution) but also has significant effects stability wise, as noted before, due to the airfoil choice.

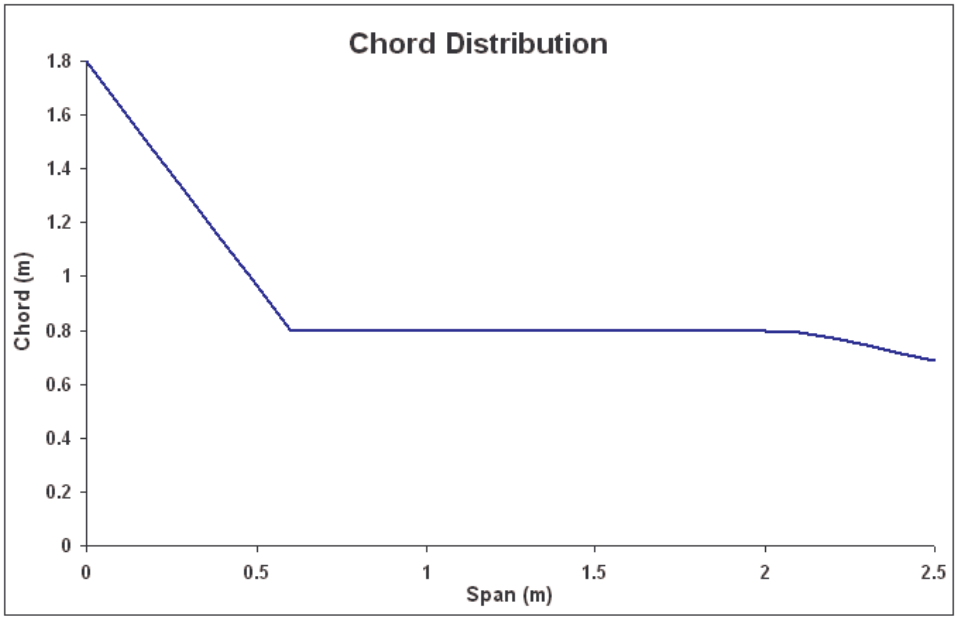

Figure 26. Spanwise chord distribution.

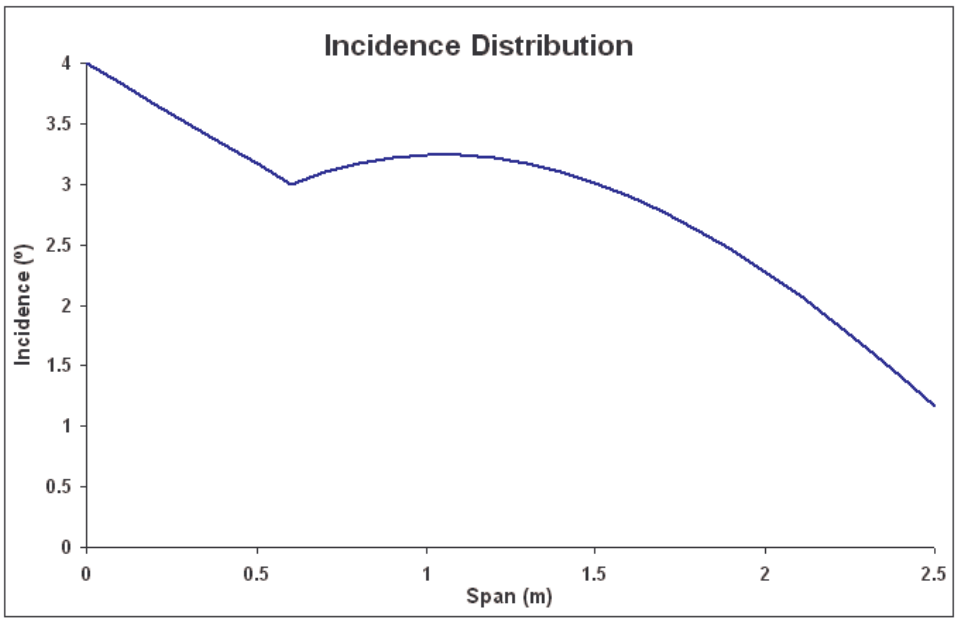

Figure 27. Spanwise incidence distribution.

VII. Conclusion

Aircraft design is an area where MDO can offer clear advantages, by exploring the interactions between all involved disciplines and taking those into account from the very beginning of the whole design process.

In this work, a number of issues were addressed in order to develop an independent MDO application.

A suitable optimization tool was investigated and developed, being the Particle Swarm Optimization algorithm the chosen one. This proved to be a suitable method, particularly for its robustness and noise insensitivity. Furthermore, any optimization algorithm that is population based is particularly suited to parallel computation, which is becoming a common reality.

Choosing a 3D Panel Method as the aerodynamic solver was based on the compromise between solution quality and computational cost, being that it is not the best aerodynamic solver available. However, given that the used code has been validated within the domain of applicability of this method, one can assume that the aerodynamic solution has enough quality to be used in this work.

Using Finite Element Method for the structural analysis guaranteed the quality of the obtained solution, in the sense that not only is the method widespread and well accepted but this also allowed to represent with good fidelity the typical aircraft structural design. Naturally, for simplicity reasons, the structural finite element model was reduced to its main components (skin panels and framed reinforcements). This model was generated from the output file of the aerodynamic solver, guaranteeing the best possible compatibility between aerodynamic and structural models.

Analyzing the obtained results, one can conclude that the optimizer tool is able to do what it is expected to: find the minima of the prescribed objective functions and therefore reach an optimal solution for the problems at hand. The developed application proved to be flexible, in the sense that it is not limited only to aircraft design, but, with the adequate models and analysis tools, can be applied to any multidisciplinary problem in the engineering field.

As for future developments, possibly one of the most interesting concepts that can be applied to this type of applications is distributed computation. The use of evolutionary algorithms is particularly suited to this strategy that can be implemented on any network of computational resources.

As for using the Artificial Neural Network as a universal approximator, it is not yet integrated in the developed application. Using real analysis to train the ANN should provide some advantages. Determining the Pareto Front is one, truly enabling the application to be a Multiobjective Multidisciplinary tool and giving designers the ability to understand the possible trade-offs that can be done along this surface. Doing this with an ANN allows approximating this surface in a very short time, if compared to obtaining the exact Pareto Front. Integrating the ANN into these applications should also allow a reduction in the computational cost of the solution, as solutions far from optimality would not be fully analyzed, only approximated in a first instance.

In order to use applications like the one developed in a real life situation, ideally, aerodynamic analyses should be performed by generating a solid model of the solution and, using CFD methods, evaluate the solution in a number of situations large enough to cover the whole flight envelope. Along with the aerodynamic solution, a highly detailed structural model should be generated, based on the typical aircraft structural elements, and the coupled aero-structural analysis performed. Obviously, to be able to do this detailed analysis a preliminary solution should be determined and that is where this work aims to be.

Other disciplines should also be included, outside of the domain of more traditional structures, aerodynamics and flight performance analysis that are done in the preliminary stage of aircraft design. Propulsion, aeroelasticity, active control of surfaces, environmental performance (fuel consumption and noise, increasingly important aspects) and operational cost, just to name a few disciplines that matter in the life cycle analysis of an aircraft, should be modeled and included in the MDO process.

Acknowledgments

Artur Fouto would like to thank his thesis supervisors Professors Alexandra Gomes and Afzal Suleman, for their supervision of this work, developed as a MSc. Thesis in Aerospace Engineering at *Instituto Superior Técnico*. This work was supported by *Fundação para a Ciência e Tecnologia* (FCT) under Grant *ICDT 05-S3T-FP012-Smorph*.

References

[1]AIAA Technical Committee on MDO, White Paper on Current State of the Art, *http://endo.sandia.gov/AIAA_MDOTC/sponsored/aiaa_paper.html* , January 1991.

[2]Joseph P. Giesing and Jean-François M. Barthelemy, A Summary of Industry MDO Applications and Needs. *At request of the AIAA Technical Committee on MDO*, 1998.

[3]S. Wakayama and I. Kroo, The Challenge and Promise of Blended-Wing-Body Optimization, *7th AIAA/USAF/NASA/ISSMO Symposium on Multidisciplinary Analysisand Optimization*, September 1998.

[4]H. Hoenlinger, J. Krammer, and M. Stettner, MDO Technology Needs in Aeroservoelastic Structural Design, *7th AIAA/USAF/NASA/ISSMO Symposium on Multidisciplinary Analysis and Optimization*, September 1998.

[5]M. H. Love, Multidisciplinary Design Practices from the F-16 Agile Falcon, *7th AIAA/USAF/NASA/ISSMO Symposium on Multidisciplinary Analysis and Optimization*, September 1998.

[6]J. Bennett, P. Fenyes, W. Haering, and M. Neal, Issues in Industrial Multidisciplinary Optimization, *7th AIAA/USAF/NASA/ISSMO Symposium on Multidisciplinary Analysis and Optimization*, September 1998.

[7]N. Radovcich and D. Layton, The F-22 Structural Aeroelastic Design Process with MDO Examples, *7th AIAA/USAF/NASA/ISSMO Symposium on Multidisciplinary Analysis and Optimization*, September 1998.

[8]N. M. Alexandrov and R. M. Lewis, Analytical and Computational Properties of Distributed Approaches to MDO, *8th AIAA/USAF/NASA/ISSMO Symposium on Multidisciplinary Analysis and Optimization*, September 2000.

[9]Ricardo M. Paiva, Development of a Modular MDO Framework for Preliminary Wing Design (MSc. Thesis). *IST*, Lisboa, 2007.

[10]J. Kennedy and R. Eberhart, Particle Swarm Optimization, *IEEE International Conference on Neural Networks, Vol. IV, pp. 1942-1948*, 1995.

[11]Ruben E. Perez and Peter W. Jansen, Aero-Structural Optimization of Non-Planar Lifting Surface Configurations, *12th AIAA/ISSMO Multidisciplinary Analysis and Optimization Conference*, September 2008.

[12]Y. Deremaux, N. Pietremont, J. Négrier, E. Herbin, and M. Ravachol, Environmental MDO and Uncertainty Hybrid Approach Applied to a Supersonic Business Jet. *12th AIAA/ISSMO Multidisciplinary Analysis and Optimization Conference*, September 2008.

[13]D. Lim, Y.-S. Ong, Y. Jin, B. Sendhoff, and B. S. Lee, Inverse multi-objective robust evolutionary design, *Springer Science & Business Media*, September 2006.

[14]Y. Jin and J. Branke, Evolutionary Optimization in Uncertain Environments – A Survey, *IEEE Transactions on Evolutionary Computation, Vol. 9, No. 3*, June.

[15]Dale L. Ashby, Michael Dudley, and Steven K. Iguchi, Development and Validation of an Advanced Low-Order Panel Method, *NASA Technical Memorandum 101024*, 1988.